ACCURACY ANALYSIS OF C/A CODE-BASED GNSS RECEIVERS IN KINEMATIC CONDITION

J. G. Sanches[1], C. E. N. Ricci[2], J.R. Regazzo.[3] S. A. Ribeiro[4], J. P. Molin[5].

[1] *Gabriel José Sanches: Mestrando em Engenharia de Sistemas Agrícolas, Escola Superior de Agricultura "Luiz de Queiroz", gabriel.sanches99@usp.br*

[2] *Carlos Eduardo Nunes Ricci: Mestrando em Engenharia de Sistemas Agrícolas, Escola Superior de Agricultura "Luiz de Queiroz", carloseduardonr@usp.br*

[3] *Jamile Raquel Regazzo: Doutoranda em Engenharia de Sistemas Agrícolas, Escola Superior de Agricultura "Luiz de Queiroz", jamile.regazzo@usp.br*

[4] *Sarah Abade Ribeiro: Mestranda em Engenharia de Sistemas Agrícolas, Escola Superior de Agricultura "Luiz de Queiroz", sarahabade@usp.br*

[5] *José Paulo Molin: Professor do Departamento de Engenharia de Sistemas Agrícolas da Escola Superior de Agricultura "Luiz de Queiroz", jpmolin@usp.br*

A paper from the Proceedings of the
17th International Conference on Precision Agriculture and 11th Brazilian Congress on Precision and Digital Agriculture
13-15 July 2026
Porto Alegre, Brazil

Abstract.

Precision agriculture has emerged as a strategic approach to optimize input use and maximize crop productivity. One of the key pillars of this practice is the collection of georeferenced data, essential for the monitoring and efficient management of cultivated areas. This study aimed to compare the performance of different positioning signal reception technologies under dynamic conditions. Three C/A code navigation receivers integrated into smartphones, one conventional navigation GPS receiver, and a GY-NEO6MV2 module were evaluated. All devices were subjected to kinematic tests performed on a pivot system with its own center of rotation, operating at speeds of 2.5 m s⁻¹ and 5 m s⁻¹, with a data collection period of 1 hour and 10 minutes for each test. A total of three tests were conducted for each speed condition, with the objective of comparing parameters such as mean error, standard deviation, accumulated error and signal stability. The results showed good consistency among the evaluated devices, with errors falling within the expected range for C/A code receivers (approximately 3 m). Although minor performance differences were observed between the devices, all demonstrated results suitable for low-precision navigation applications.

Keywords: *GNSS, C/A code, kinematic, accuracy, ESP32*

1 Introduction

The use of GNSS (Global Navigation Satellite System) receivers has expanded in agriculture, more specifically within the context of precision agriculture, which is fully dependent on high-quality georeferenced information with increasingly higher levels of precision and accuracy. The effectiveness of these operations is directly associated with factors such as the quality of the GNSS receivers, the availability and integrity of the signals, and the effects of atmospheric interference, especially that caused by the ionosphere. These variables can affect positioning accuracy, producing significant impacts on systems that rely on real-time data or on surveys requiring high positional reliability.

According to Pérez-Ruiz and Upadhyaya (2012), GNSS positioning can be carried out by different methods, each with distinct operational characteristics, levels of complexity and precision. Single Point Positioning (SPP), for instance, relies exclusively on the C/A code (Coarse/Acquisition code), a freely accessible signal transmitted on the L1 frequency by the satellites of the GPS constellation. This method computes the user position from the pseudoranges between the receiver and the visible satellites, offering typical precision on the order of metres. For applications that require higher accuracy, techniques such as DGNSS, SBAS, PPP (Precise Point Positioning) and RTK (Real Time Kinematic) are widely used.

According to Rosalen et al. (2010), even with limitations in terms of accuracy, the use of GNSS receivers based on the C/A code has been consolidated in several precision agriculture activities, such as soil sampling, georeferencing of areas and the construction of management zones. However, these applications require specific evaluations to verify whether the level of precision achieved is compatible with the requirements of agricultural operations.

The demand for precision in GNSS receivers varies according to the agricultural operation to be performed, making it essential to study the behaviour of these devices in real use environments (Maldaner et al. 2021). Several studies have been conducted to evaluate the accuracy and precision of different equipment under controlled conditions, as reported by authors such as Stabile and Balastreire (2006), Machado and Molin (2011), Trevisan et al. (2014), Passalaqua et al. (2015), Lopes (2016), Rodrigues (2017) and Maldaner et al. (2021).

Thus, the present study aimed to compare, in kinematic field tests, the data obtained by navigation receivers embedded in smartphones, a navigation GPS and a GNSS module, all of them classified as C/A code GNSS receivers.

According to Maldaner et al. (2021), the evaluation of GNSS receivers under static and dynamic conditions requires the application of rigorous statistical parameters to quantify their precision and reliability. In this study, statistical metrics such as the mean error, the standard deviation and the 95% confidence error (2σ) were used. These metrics were computed by comparing the data obtained by the GNSS receivers with a previously known circular reference trajectory followed by the pivot during its rotational movement.

2 Material and Methods

The tests were carried out in an area of the Precision Agriculture Laboratory at the Department of Biosystems Engineering of USP/ESALQ, in the municipality of Piracicaba, SP, Brazil (22º 42′ 48.32″ S, 47° 37′ 42.45″ W; altitude of 540 m), between 23 and 25 April 2025. Three GNSS receivers using the L1 signal were employed, with communication by C/A code and internal data storage capability: a GY-NEO6MV2 module (u-blox, Thalwil, Switzerland), a Samsung Galaxy S20 FE 5G smartphone (Samsung Electronics, Suwon, South Korea) and a Garmin eTrex Legend HCx handheld GPS (Garmin Ltd., Olathe, KS, USA).

The data were collected with the devices positioned on a platform fixed to a pivot whose central point had coordinates 22° 42′ 48.17276″ S and 47° 37′ 42.84343″ W, named "Base Point". The kinematic test was performed using a methodology similar to that of Maldaner et al. (2021). The receivers placed on the platform were positioned 10.23 m from the end of a truss structure free to rotate around the georeferenced central pivot, so that this information was used to create the reference trajectory circle, subsequently used to compute the distance between the points collected by the devices.

Three replicates were performed for two tangential rotation speeds, 2.5 m s^{-1} and 5.0 m s^{-1}, both under a Uniform Circular Motion (UCM) regime. All receivers collected data at a frequency of 0.2 Hz (one record every 5 s), with each replicate lasting 1 h 10 min, discarding the first 5 min and the last 5 min, and providing an interval of at least 20 min between collections, as shown in Table 1. Owing to adverse weather conditions (rain), it was not possible to perform the three consecutive collections at the speed of 2.5 m s^{-1}. To compose the three tests required for each speed, a test collection previously carried out on 23 April 2025 at a speed of 2.5 m s^{-1} was used. This collection was included in Table 1 as Replicate 6 and is duly highlighted.

Table 1 Tests performed

Replicate	**Speed (m s^{-1})**	**Date**	**Start**	**End**
1	5	25/04/25	9:20	10:30
2	5	25/04/25	10:50	12:00
3	5	25/04/25	12:25	13:35
4	2.5	25/04/25	13:58	15:08
5	2.5	25/04/25	15:50	17:00
6(*)	2.5	23/04/25	15:51	17:01

(*) Test collection performed previously

Fig. 1 Positioning of the receivers on the platform mounted at the end of the pivot

The data were exported in CSV format. The data from the Garmin required cleaning with Microsoft Excel software (Microsoft Corp., Redmond, WA, USA), as they contained disorganized headers that prevented them from being opened for analysis in a programming environment.

2.1 Equipment specifications

The Garmin eTrex Legend HCx GNSS receiver (Garmin Ltd., Olathe, KS, USA), a navigation receiver with L1 signal and C/A code shown in Fig. 2, is a portable, compact and rugged device that works only with the GPS (Global Positioning System) and up to 12 simultaneous channels. Classified as an entry-level model, it has limitations that restrict its use in precision agriculture applications. According to the manufacturer manual, its positional precision ranges between 3 and 5 m, with an acquisition rate of one reading per second, a performance insufficient to meet the accuracy levels required in more advanced operations. On the other hand, it stands out for features such as water resistance (IPX7 rating) and an autonomy of up to 25 h of operation using only two AA batteries.

Fig. 2 Garmin eTrex Legend HCx navigation device used in the collections

The second device selected was the Samsung Galaxy S20 FE 5G smartphone (Samsung Electronics, Suwon, South Korea), which features a Qualcomm Snapdragon 865 (SM8250) processor with integrated support for GNSS systems such as GPS, GLONASS, Galileo, BeiDou, QZSS and SBAS, using the internet and cellular towers to assist signal acquisition.

For data acquisition, the SW Maps application was used, as illustrated in Fig. 3. This application allows logging of latitude and longitude associated with the respective collection times. In addition, it offers functionalities such as track segmentation and has an intuitive interface, facilitating both field operation and the export of the collected data.

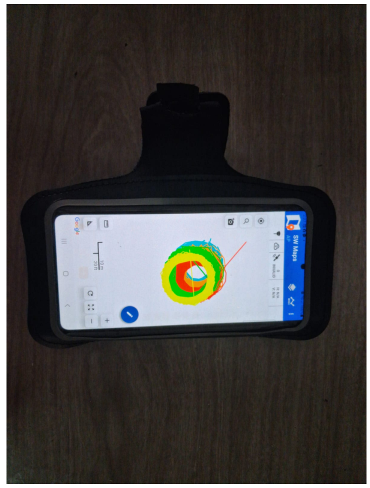

Fig. 3 Samsung Galaxy S20 FE 5G smartphone used in the collections

Finally, in order to assess the feasibility of using IoT devices in agriculture, a GY-NEO6MV2 module (u-blox, Thalwil, Switzerland) was used, which supports only NAVSTAR GPS, with 50 simultaneous channels. It was coupled to an ESP32-WROOM (Espressif Systems, Shanghai, China) through the UART communication protocol with a transmission rate of 9600 bps, both connected by means of an 890-point breadboard to establish the electrical connection of the modules and the microcontroller, together with cables at 3.3 V. The assembly was housed inside a blue plastic container, as shown in Fig. 4.

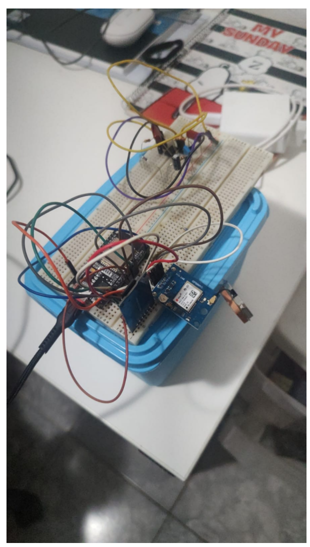

Fig. 4 ESP32 and GNSS module used in the coordinate collection

Fig. 5 presents the schematic diagram of the IoT system, based on the ESP32 microcontroller, which communicates with two modules: a GPS module (GY-NEO6MV2) and an SD card reader. The GPS module transmits data via the UART protocol, using pins GPIO 16 (RX2) and GPIO 17 (TX2) of the ESP32 (Serial 2), and the data recording on the SD card is performed through the SPI interface.

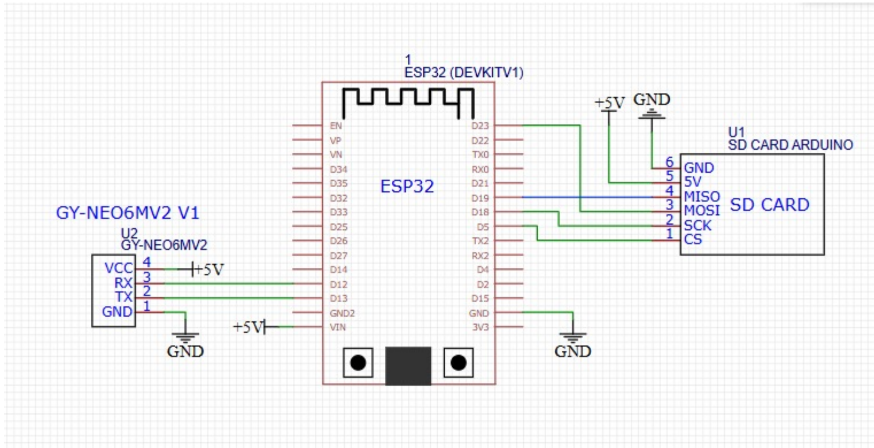

Fig. 5 Schematic model of the IoT equipment assembly

As it is an IoT device, its programming had to be developed. For this purpose, Visual Studio Code software was used together with the PlatformIO extension for the development and compilation of the C++ code, available on GitHub: https://github.com/GabrielSan99/GNSS_C-A_CODE (last accessed 4 June 2026). Owing to the use of the modules, the TinyGPSPlus and SD libraries were added for the correct operation of the code.

2.2 Evaluation metrics

The kinematic configuration of the tests, combined with the limitations of the equipment used, does not allow the exact point where each GNSS reading should have occurred to be determined precisely. This is due to the fact that all receivers installed on the pivot platform operate exclusively with the C/A code signal on the L1 frequency, which compromises the accuracy of the measurements in motion.

Given this limitation, metrics widely used in the literature for evaluating the precision of GNSS receivers in kinematic applications were adopted. The positioning error was determined based on the geodesic distance between the recorded point and the centre of the pivot, considering a known reference radius.

To compute these distances, the geopy library of Python was used, considered reliable according to Lawhead (2019), which operates based on the WGS-84 ellipsoidal model, implementing robust geodesic methods such as the Vincenty formula or Great Circle. This procedure ensures higher precision in the conversion of geographic coordinates into metres, even over relatively short distances, as is the case in this experiment.

The individual error E_i was defined as the difference between the computed distance (d_i) and the pivot reference radius (R = 10.23 m), as expressed by Eq. 1 and by Fig. 6, which presents the geometric configuration of the experiment.

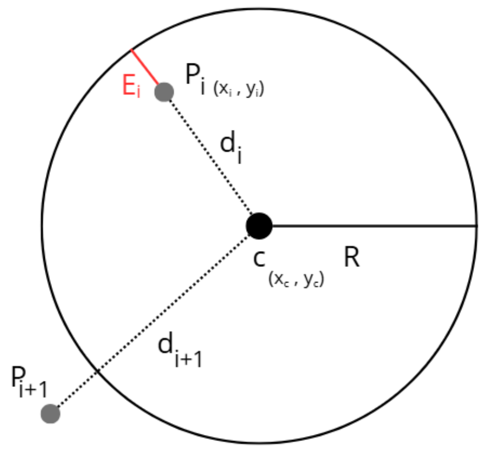

Fig. 6 Model for error computation

$$E_i = d_i - R \qquad (1)$$

The Mean Error (ME) was then computed as the average of the individual errors for each observation and situation analysed, according to Eq. 2, where *n* is the number of observations.

$$ME = \frac{1}{n}\sum_{i=1}^{n} E_i \qquad (2)$$

With the ME previously computed, it was possible to determine other statistical metrics important for this type of experiment, such as the standard deviation, represented by σ (Eq. 3), and the value of 2σ, a relevant metric that represents the range of variation in which 95% of the data lie in a normal distribution.

$$\sigma = \sqrt{\frac{1}{n}\sum_{i=1}^{n}(E_i - ME)^2} \qquad (3)$$

3 Results and Discussion

The following results were organized based on the experimental design adopted, which considered two main factors: travel speed of the central pivot and replicate. The first three replicates (1 to 3) were conducted at a speed of 5.0 m s^{-1}, whereas the subsequent replicates (4 to 6) were performed at a speed of 2.5 m s^{-1}. The analysis aimed to compare the positional performance of the three GNSS receivers evaluated — Garmin, Smartphone and ESP32 — in each test condition, considering statistical metrics such as the radial mean error (ME), the standard deviation (SD) and the confidence interval of twice the standard deviation (2σ).

3.1 Experiments at 5 m s^{-1}

The points recorded by the GNSS receivers were plotted using the Matplotlib library of Python (Fig. 7), together with the reference circle that represents the ideal coordinates to be recorded. This visualization made it possible to identify possible outliers and behaviour patterns in the data distribution. An atypical deviation was observed, for example, in replicate 3 for the data obtained by the ESP32, indicating the occurrence of a possible problem with the receiver used together with the microcontroller. Even so, these data were kept in the computation of the evaluation metrics, since such behaviour highlights the limitation of the system in maintaining reliable performance over time.

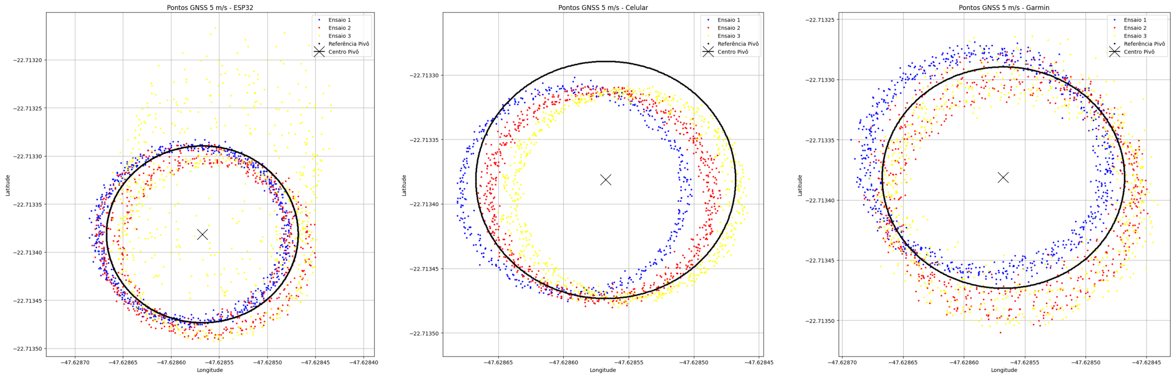

Fig. 7 Scatter of the points for replicates at 5 m s⁻¹: a replicate 1; b replicate 2; c replicate 3

The evaluation metrics, presented in Table 2, show that the atypical scatter observed in replicate 3 for the receiver coupled to the ESP32 (highlighted with "a") negatively affected the results, generating values up to three times higher than those obtained in replicates 1 and 2. On the other hand, the other devices maintained more consistent results among the three replicates, indicating greater stability in data acquisition.

Table 2 Results of the replicates at 5 m s⁻¹

Replicate	Device	ME	SD	2 σ
1	ESP32	0.706	0.444	0.889
1	Smartphone	1.845	1.321	2.641
1	Garmin	1.308	0.743	1.485
2	ESP32	1.014	0.609	1.219
2	Smartphone	1.350	0.964	1.929
2	Garmin	1.095	0.837	1.674
3	ESP32 (a)	2.955	2.731	5.461
3	Smartphone	1.522	1.146	2.292
3	Garmin	1.459	0.974	1.948

(a) Highest uncertainty indices. Values in metres

To complement the results presented in Table 2, the error values were represented graphically in Fig. 8 and Fig. 9, allowing a clearer visual analysis of the data distribution and showing that the highest concentration lies between 1 and 3 m for the replicates that occurred under normal conditions, with maximum values of 5 m, differently from replicate 3 for the ESP32, which presents values recorded above 10 m.

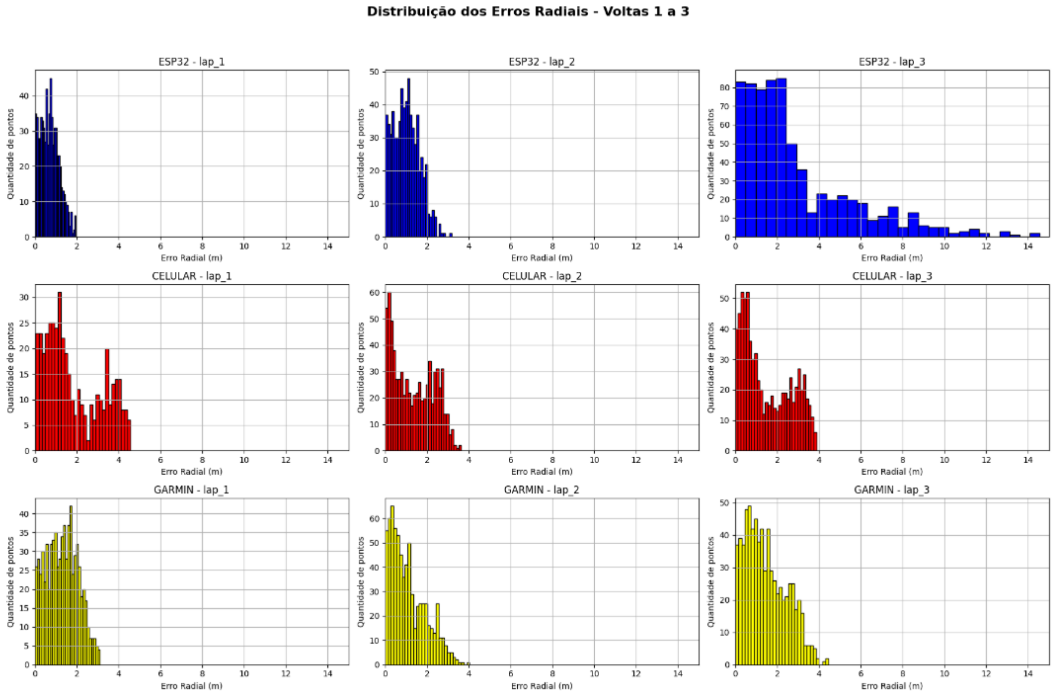

Fig. 8 Error distribution for replicates at 5 m s⁻¹

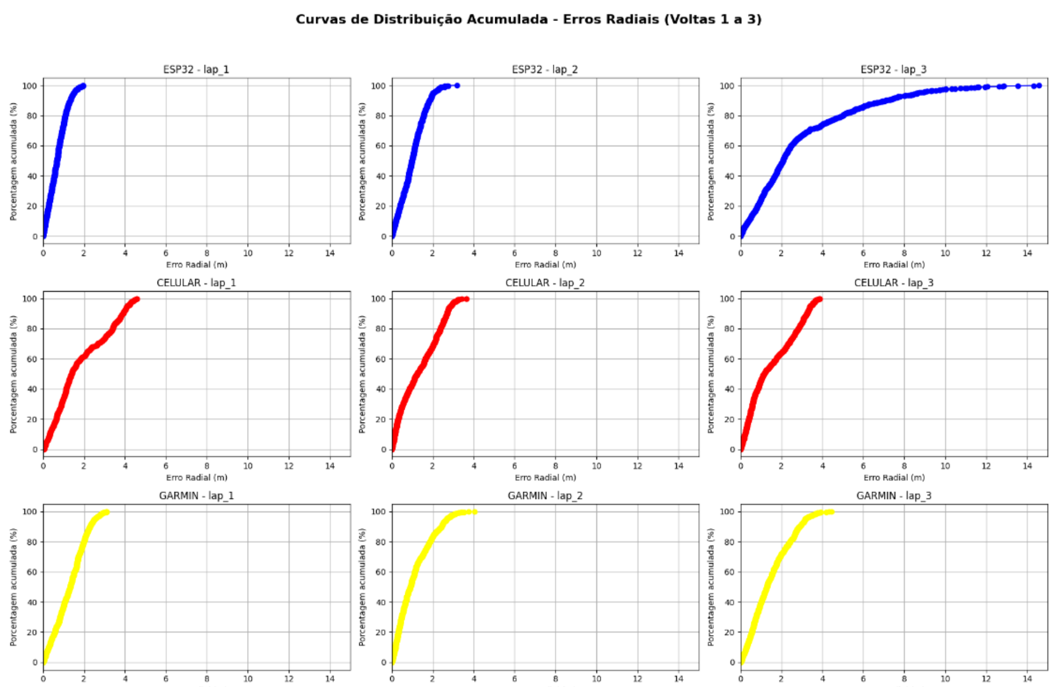

Fig. 9 Cumulative error distribution for replicates at 5 m s⁻¹

Finally, the averages of the evaluation metrics were computed for each device, based on the data obtained from the three replicates. This allowed a more direct numerical comparison between the devices, as presented in Table 3, in which the values closest to zero are highlighted with "a". Thus, the Garmin receiver showed the best performance among the evaluated devices, presenting the lowest mean error (ME) values and the lowest standard deviations across the replicates, which indicates that the device was simultaneously more precise and more accurate under the experimental conditions analysed.

Table 3 Mean of the results of the replicates at 5 m s⁻¹

Device	ME	SD	2σ
ESP32	1.559	1.595	3.190
Smartphone	1.572	1.144	2.287
Garmin (a)	1.287	0.852	1.704

(a) Lowest uncertainty indices. Values in metres

3.2 Experiments at 2.5 m s⁻¹

The same analytical procedure was carried out for replicates 4, 5 and 6, whose speed was 2.5 m s⁻¹. Fig. 10 shows the scatter of the points, which visually appear more dispersed than for the speed of 5 m s⁻¹ and with a tendency of displacement towards the southeast direction in all replicates and for the three receivers. This displacement differs from that observed in replicate 3 for the ESP32, given that all experiments follow the same displacement tendency in the NW-SE direction and do not present points recorded outside a circular pattern.

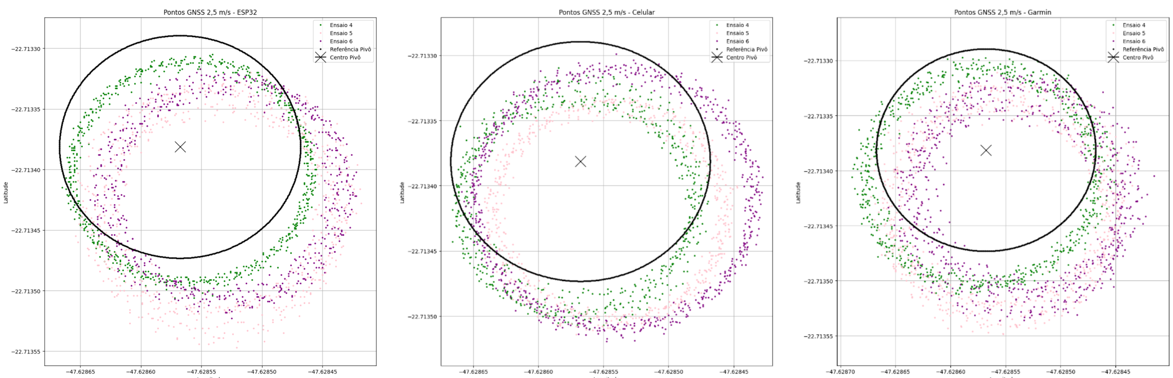

Fig. 10 Scatter of the points for replicates at 2.5 m s⁻¹: a replicate 4; b replicate 5; c replicate 6

Table 4 presents the evaluation metrics used and shows, once again, that the ESP32 was the device with the highest uncertainty levels. It is important to highlight that the displacement that occurred during the tests contributed to the increase in the error values for all devices in the replicates analysed.

The increase in the error values proved to be inconsistent with what was expected, since, according to Ji et al. (2022), higher speeds tend to generate higher uncertainty indices due to the Doppler effect. This result indicates the need to perform a larger number of replicates per speed, as well as to test a wider range of speeds. The difference between the analysed speeds (2.5 m s⁻¹ and 5 m s⁻¹) may not have been sufficient to reveal the expected behaviour. In addition, the observed results may have been influenced by other factors, such as the availability and geometry of the satellites at the time of the collections.

Table 4 Results of the replicates at 2.5 m s⁻¹

Replicate	Device	ME	SD	2σ
4	ESP32	1.624	0.852	1.704
4	Smartphone	2.168	1.386	2.773
4	Garmin	1.891	1.077	2.155

Replicate	Device	ME	SD	2σ
5	ESP32 (a)	4.028	2.151	4.303
5	Smartphone	3.033	1.649	3.298
5	Garmin	3.784	2.017	4.035
6	ESP32	3.441	1.794	3.588
6	Smartphone	2.794	1.492	2.985
6	Garmin	3.640	1.920	3.840

(a) Highest uncertainty indices. Values in metres

The error distribution also increased, as shown by Fig. 11 and Fig. 12, so that the errors are concentrated between 1 and 5 m, but this time without the presence of error values that deviate from the experimental patterns.

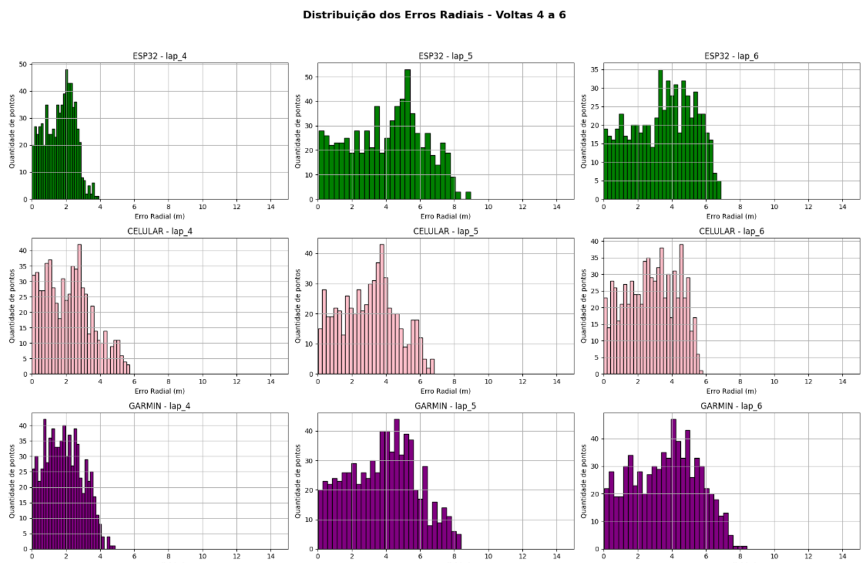

Fig. 11 Error distribution for replicates at 2.5 m s⁻¹

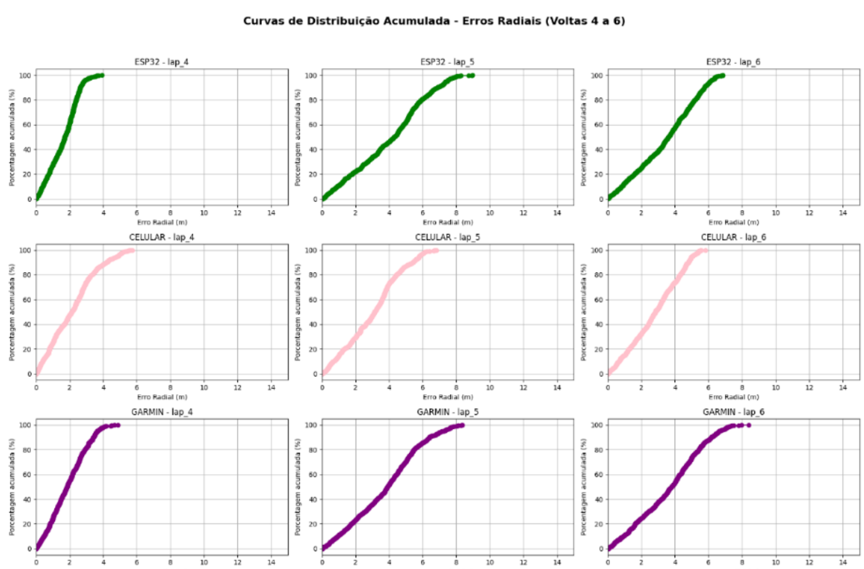

Fig. 12 Cumulative error distribution for replicates at 2.5 m s^{-1}

For the experiments conducted at the speed of 2.5 m s^{-1}, the smartphone was recorded as the receiver with the lowest uncertainty index (Table 5).

Table 5 Mean of the results of the replicates at 2.5 m s^{-1}

Device	ME	SD	2σ
ESP32	3.031	1.599	3.198
Smartphone (a)	2.665	1.509	3.018
Garmin	3.105	1.672	3.343

(a) Lowest uncertainty indices. Values in metres

4 Conclusion

This work presented a comparative analysis of the performance of three GNSS receivers based on the C/A code: the GY-NEO6MV2 IoT module with ESP32, the Garmin handheld GPS and the GPS of the Samsung Galaxy S20 FE 5G smartphone. The evaluations were performed in circular motion, at speeds of 2.5 m s^{-1} and 5.0 m s^{-1}, aiming to verify the precision and reliability of the devices in applications typical of precision agriculture.

The results indicated that all devices presented mean errors on the order of metres, compatible with the limitations of the C/A code on the L1 frequency. The Garmin eTrex Legend HCx showed the best performance in terms of precision and stability, especially under the higher speed conditions, presenting the lowest mean error and the lowest standard deviation among the replicates. The smartphone also showed satisfactory performance, although with greater variability, while the IoT module showed greater instability, especially in one of the replicates performed.

The influence of speed on the precision and accuracy of the receivers was not directly confirmed, since, for the lower speed, the errors recorded were higher, which does not agree with the literature. That said, it is proposed to perform tests at at least five different speeds, in order to analyse the relationship between speed and precision, and to conduct experiments involving Uniformly Varied Circular Motion (UVCM), with the aim of evaluating how the error behaves in response to variations in angular acceleration.

In conclusion, the study demonstrated that, despite using the same type of signal, the GNSS receivers present small performance differences, which should be considered in the choice of equipment for agricultural applications. Furthermore, the potential of IoT modules for low-cost solutions was evidenced, although they still require improvements to achieve the reliability required in dynamic operations.

References

Ji, L., Sun, R., Cheng, Q., & Wang, J. (2022). Evaluation of the performance of GNSS-based velocity estimation algorithms. *Satellite Navigation, 3*(1), 1–13. doi:10.1186/s43020-022-00063-9

Lawhead, J. (2019). *Learning geospatial analysis with Python* (3rd ed.). Birmingham, UK: Packt Publishing.

Lopes, T. G. (2016). *Avaliação de desempenho de um sistema híbrido de GPS incorporado a dispositivos móveis para a obtenção de levantamentos planimétricos com fins agrícolas* (Undergraduate thesis). Instituto Federal de Educação, Ciência e Tecnologia Farroupilha /

Universidade Federal do Pampa, Alegrete, Brazil.

Machado, T. M., & Molin, J. P. (2011). Ensaios estáticos e cinemáticos de receptores de GPS. *Revista Brasileira de Engenharia Agrícola e Ambiental, 15*(9), 981–988.

Maldaner, L. F., Canata, T. F., Dias, C. T. S., & Molin, J. P. (2021). A statistical approach to static and dynamic tests for Global Navigation Satellite Systems receivers used in agricultural operations. *Scientia Agricola, 78*(5), e20200023.

Passalaqua, B. P., Maldaner, L. F., Canata, T., & Molin, J. P. (2015). Avaliação da precisão dos sinais RTK e RTK em rede em ensaio estático e cinemático. In *X Congresso Brasileiro de Agroinformática*. Ponta Grossa, Brazil.

Pérez-Ruiz, M., & Upadhyaya, S. K. (2012). GNSS in precision agricultural operations. *Applied Engineering in Agriculture, 28*(6), 727–739. doi:10.13031/2013.42497

Rodrigues, J. P. C. S. (2017). *Análise comparativa de receptores de posicionamento por satélite para levantamento planimétrico de imóveis rurais* (Undergraduate thesis). Universidade Federal da Paraíba, Areia, Brazil.

Rosalen, D. L., Takahashi, K. M., & Gonçalves, K. C. (2010). Avaliação da precisão, tendência e acurácia de receptores GPS de navegação para fins de agricultura de precisão. In *Congresso Brasileiro de Agricultura de Precisão*. Ribeirão Preto, Brazil.

Stabile, M. C. C., & Balastreire, L. A. (2006). Comparação de três receptores GPS para uso em agricultura de precisão. *Engenharia Agrícola, 26*(1), 215–223.

Trevisan, R. G., Eitelwein, M. T., Vilanova Jr., N. S., Salvi, J. V., Passalaqua, B. P., & Molin, J. P. (2014). Avaliação da precisão dos sinais RTK e RTX em ensaio estático e cinemático. In *Congresso Brasileiro de Agricultura de Precisão*. São Pedro, Brazil.